In-medium properties of vector mesons: nucleonic resonances effects *

M.D. Cozma
National Institute for Physics and Nuclear Engineering
Atomiştilor 407, 077125 Măgurele-Bucharest, Romania

Dileptons represent a unique probe for nuclear matter under extreme conditions reached in heavy-ion collisions allowint the study of meson properties, like mass and decay width, at various density and temperature regimes. These phenomena are thought to be precursors of the phase-transition of strongly interaction matter from the hadron gas phase to a phase in which quarks are deconfined and chiral symmetry is restored, known as quark-gluon plasma. We employ the extended vector meson dominance (eVMD) model to determine the spectral functions of vector mesons in nuclear matter and use this information to simulate the dilepton spectrum in collisions of light nuclei. Furthermore, the dependence of the theoretical predictions on model input data and assumptions on momentum distribution of nucleons in the heavy-ion collision fireball is studied.

I. INTRODUCTION

Dileptons produced in heavy ion reactions present an unique opportunity for the study of nuclear matter under extreme conditions, providing a clear view on effective degrees of freedom at high baryon density and temperature. It has been argued that their differential spectra could reveal information about chiral restoration and in-medium properties of hadrons [1–3]. Theoretically, there exists an abundance of models that predict a change of vector meson masses and widths in high density/temperature nuclear matter: Brown-Rho scaling [1] is equivalent with a decrease of vector meson masses in nuclear medium; models based on QCD sum rules [2] and effective hadronic models [4–9] reach similar conclusions.

Experimentally, a significant enhancement of the dilepton spectrum in low energy heavy ion collisions [10, 11] over the known hadronic sources has been observed. This could not be explained by present models, as opposed to the ultrarelativistic case, even when the in-medium spectral functions or the dropping mass scenarios are taken into account [12, 13]. Other scenarios like contributions from quark-gluon plasma, in-medium modifications of the η mass or decoherence effects [14] have proved only partially successful. Recent results [15] on dimuon spectra with high resolution in the vicinity of the ρ-ω peak seem to rule out a naive dropping mass scenario but support the picture of modified $\rho - \omega$ spectral functions. Dilepton spectra with unprecedented mass resolution for the reactions A+A, p+A and π+A will be available from the HADES Collaboration at GSI [16] in the near future, allowing the extraction of in-medium properties of the ρ and ω vector mesons.

The resonance model developed by the group in Tübingen and collaborators [17–19] describes, among other reactions, vector meson production through the decay of nucleonic resonances, a prerequisite for the description of vector mesons in nuclear matter. Section II of this report is dedicated to a calculation of the ρ and ω in-medium spectral functions together with a minimal list of details regarding the eVMD model and its application to dilepton emission. In Section III we focus on a study regarding uncertainties in the theoretical dilepton-spectrum as well as in-medium vector meson spectral functions resulting from the model input data together with the assumptions on the momentum distribution of nucleons in the fireball. We end with a comparative study on the effect of in-medium vector meson properties on the dilepton spectrum in collisions of light nuclei, treated in a traditional way (a la Brown-Rho) and through spectral functions (Section IV).

II. THE MODEL

A. The Extended VMD model

In this Section we review those ingredients of the eVMD model [18] of interest for the discussion to follow. The aim of the model is the description of the electromagnetic transition current between a nucleon and a nucleonic resonance

---

* This document represents a progress report for the project "Hadron Properties in Nuclear Matter and Dilepton Emission in Relativistic Heavy-Ion Collisions" (project code: RP9) due on December 15^{th} 2007.

of spin J. It can be formerly written as follows

$$J_\mu(p_R,\lambda_R,p,\lambda) \;=\; e\,\bar{u}_{\beta_1\ldots\beta_2}(p_R,\lambda_R)\,\Gamma^{(\pm)}_{\beta_1\ldots\beta_2\mu}u(p,\lambda), \tag{1}$$

with m_R and m denoting the masses of the nucleonic resonance and nucleon respectively, λ_R and λ are their corresponding helicities and the upper index $\pm$ denotes a resonance of normal and abnormal parity respectively. Making use of Lorentz covariance, the vertex operator $\Gamma^{(\pm)}_{\beta_1\ldots\beta_2\mu}$ can be written, in its most general form, as

$$\begin{aligned}\Gamma^{(\pm)}_{\beta_1\ldots\beta_2\mu} &= q_{\beta_1}\cdots q_{\beta_{l-1}}\,\Gamma^{(\pm)}_{\beta_l\,\mu}\\ \Gamma^{(\pm)}_{\beta,\mu} &= \sum_k \Gamma^{(\pm)\,k}_{\beta\,\mu}\,F^{(\pm)}_k\,.\end{aligned} \tag{2}$$

Here, q denotes the momentum of the emitted (or absorbed) photon. The Dirac structure of the interaction vertexes is fully absorbed in the matrices $\Gamma^{(\pm)\,k}_{\beta\mu}$, while the scalar functions $F^{(\pm)}_k$, called covariant form-factors contain the dynamics. In the case of the eVMD only the operators $\Gamma^{(\pm)\,k}_{\beta\mu}$ which give a non-zero contribution on-shell are considered, which reduces their number at 2 (for spin 1/2 resonances) and 3 (for spin 3/2 and higher resonances). Their actual expressions can be found in [18].

In the vector meson dominance model the coupling of photons to hadrons, and in particular to the nucleon-resonance system, is supposed to take place via the exchange of a intermediate vector meson in the original version and a vector meson and its excited states in the extended one, which implies the following form for the electromagnetic current: $J_\mu = -e\sum_V \frac{m_V^2}{g_V}\,V_\mu$, where V_μ denotes the vector meson field operator and the factor in front of it is a consequence of electric charge universality. With this assumption it is not difficult to see that the covariant form factors can be put in the form

$$F^{(\pm)}_k(q^2) \;=\; \sum_V \frac{f^{(\pm)}_{VNR,k}}{g_V}\,\frac{1}{1-q^2/m_V^2}. \tag{3}$$

The asymptotic form of the covariant form-factors is fixed using quark-model arguments (known as quark-counting rules, see [23]) fixing not only the minimum number of intermediate vector mesons needed, but also reducing the number of free parameters (meson-nucleon-resonance couplings). Consequently, the expressions for the form-factors can be written as

$$F^{(\pm)}_1(q^2) = \frac{\sum_{j=0}^{n+1} C^{(\pm)}_{1j}\,q^{2j}}{\prod_{i=1}^{l+3+n}(1-q^2/m_i^2)}\,, \qquad F^{(\pm)}_{2,3}(q^2) = \frac{\sum_{j=0}^{n} C^{(\pm)}_{2,3j}\,M^{2j}}{\prod_{i=1}^{l+3+n}(1-q^2/m_i^2)}, \tag{4}$$

with $l+3+n$ the number of vector mesons ($l+1/2$ being the spin of the resonance under consideration). This expression is equivalent with Eq. (3) in the no-width approximation. Finally, the couplings $C_{1,2,3j}$ are fitted to the "experimental" values for the helicity amplitudes $A_{3/2}$, $A_{1/2}$ and $S_{1/2}$ which can be defined by suitable labeling the contraction of Eq. (1) with the photon polarization four-vector.

B. Vector mesons in nuclear medium

Properties of elementary particles in vacuum as well as in a nuclear medium are encoded in the two-point function $\langle\Omega|T(V_\mu(x)V_\nu(y))|\Omega\rangle$ also known as the propagator. One starts from the expression of the free-propagator, which in the case of a spin-1 particle (ρ or ω vector meson) can be put in the form

$$D^0_{\mu\nu}(k) \;=\; \frac{-g_{\mu\nu}+k_\mu k_\nu/k^2}{k^2-m^2+i\varepsilon} + \frac{1}{m^2}\frac{k_\mu k_\nu}{k^2}\,. \tag{5}$$

Due to self-interactions and scattering off particles in a dense medium the free propagator is modified, the two-point function receives higher order contributions which are generically accounted for in the self-energy $\Sigma_{\mu\nu}$. Making use of Lorentz covariance the most general expression for the self-energy reads

$$\Sigma_{\mu\nu}(k,n) = g_{\mu\nu}\,\Sigma_1(k,n) + k_\mu\,k_\nu\,\Sigma_2(k,n) + n_\mu\,n_\nu\,\Sigma_3(k,n) + k_\mu\,n_\nu\,\Sigma_4(k,n)\,, \tag{6}$$

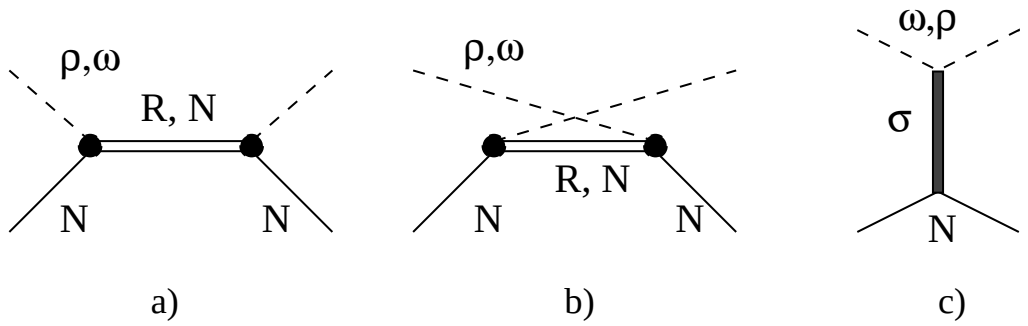

FIG. 1: Diagrammatic representation of processes contributing to the in-medium vector meson self-energies: a) direct Compton and b) crossed Compton scattering of mesons on nucleons with (R) and without (N) excitation of nucleonic resonances; c) scattering of vector mesons off nucleons with the exchange of a σ mesons.

which in the special case of gauge invariant interactions can be simplified to

$$\begin{aligned} \text{in vacuum} \;:\; & \Sigma_{\mu\nu} = P^T_{\mu\nu}(k)\,\Sigma_{vac}(k) \\ \text{in medium} \;:\; & \Sigma_{\mu\nu} = T_{\mu\nu}\,\Sigma^T(k) + L_{\mu\nu}\,\Sigma^L(k)\,. \end{aligned} \tag{7}$$

Here the $P^T_{\mu\nu}, T_{\mu\nu}$ and $L_{\mu\nu}$ are projectors on the four-dimensional transverse, three-dimensional transverse and respectively longitudinal degrees of freedom whose expressions can be found elsewhere. The four-vector n_μ characterizes the properties of nuclear nuclear matter in an arbitrary rest-frame and reduces to $(m_N,\,\vec{0})$ in its rest frame. The above expression for the self-energy allows the summation of the perturbative solution of the Dyson-Schwinger equation for the spin-1 propagator, to arrive at the final expression

$$D_{\mu\nu}(k) = -\frac{L_{\mu\nu}(k)}{k^2 - m^2 - \Sigma^L(k^2)} \;-\; \frac{T_{\mu\nu}(k)}{k^2 - m^2 - \Sigma^T(k^2)} + \frac{1}{m^2}\,\frac{k_\mu k\nu}{k^2}\,. \tag{8}$$

The spectral function, defined as the imaginary part of the propagator, contains all the relevant information about particle properties, such as pole mass and decay widths, in nuclear matter. For the case of spin-1 mesons, due to the fact that manifest Lorentz covariance is broken in nuclear medium, one has to deal with two such spectral functions characterizing separately the longitudinal and transversal degrees of freedom

$$A^{L,T}(k,n) = -\frac{1}{\pi}\,\frac{-\mathcal{I}m\,\Sigma^{L,T}(k,n)}{(k^2 - m_V^2 - \mathcal{R}e\,\Sigma^{L,T}(k,n))^2 + (-\mathcal{I}m\,\Sigma^{L,T}(k,n))^2}\,. \tag{9}$$

Eventhough not stated explicitly, self-energies, and implicitly also spectral functions, depend independently on k^0 and $\vec{k}$ at finite nuclear matter densities as effect of the finite Fermi momentum p_F. The longitudinal and transversal part of the meson self-energies each can be written as the sum of a vacuum term and a medium contribution: $\Sigma^{L,T}(k,n) = \Sigma^{L,T}_{vac}(k,n) + \Sigma^{L,T}_{med}(k,n)$. The vacuum contribution is conventionally defined as being purely imaginary, the real part being implicitly absorbed in the mass term that defines the pole mass m_V of the meson in vacuum, $\Sigma^{L,T}_{vac}(k,n) = -i\,\sqrt{k^2}\,\Gamma_{vac}$ (see [24] for the energy dependence parametrization of vacuum decay widths of ρ and ω vector mesons).

In our model, a few contributions to vector mesons self-energies in nuclear matter have been considered. First we discuss contributions due to excitation of nucleon resonances. For simplicity we will consider a schematic model of a spin 1/2 resonance which is excited by the absorption of a vector meson (of isospin 0) by a nucleon: $\mathcal{L}_{int} = -g\overline{\psi}_R\,\Gamma^\mu\,\psi\,V_\mu$. There are two contributions to the self-energy tensor originating from the direct and crossed contributions to the Compton scattering of mesons off nucleons (Fig. (1)a)-b)):

$$\Sigma^{R\,(direct)}_{\mu\nu} \;=\; \int_{|\vec{p}|<p_F} d^3\vec{p}\;\mathrm{Tr}\,\big[\,\frac{\not{p}+m_N}{2m_N}\,\Gamma^*_\mu\,\frac{\not{p}+\not{k}+m_R}{(p+k)^2 - m_R^2 + i\,m_R\,\Gamma_R}\,\Gamma_\nu\,\big]\,, \tag{10}$$

$$\Sigma^{R\,(crossed)}_{\mu\nu} \;=\; \int_{|\vec{p}|<p_F} d^3\vec{p}\,\mathrm{Tr}\,\big[\,\frac{\not{p}+m_N}{2m_N}\,\Gamma^*_\nu\,\frac{\not{p}-\not{k}+m_R}{(p-k)^2 - m_R^2 + i\,m_R\,\Gamma_R}\,\Gamma_\mu\,\big]\,. \tag{11}$$

where at first order in a density expansion, nucleon and resonance propagators are unaffected by the presence of the dense nuclear medium. The parameters m_R and Γ_R stand for the mass and respectively decay width of the nucleonic

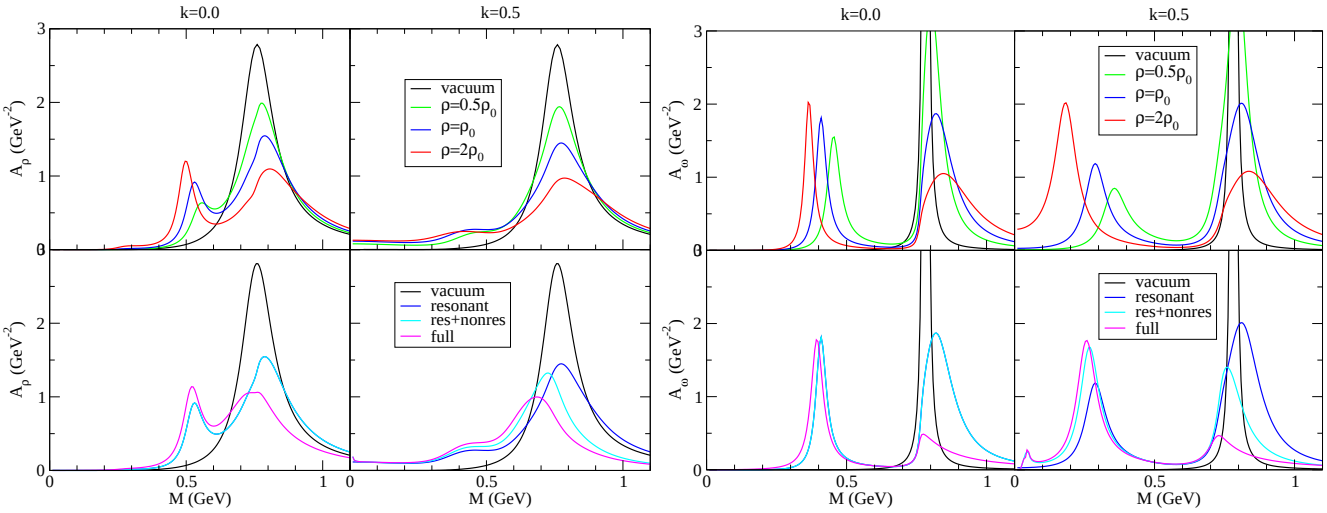

FIG. 2: Averaged spectral functions of the ρ (left plot) and ω (right plot) vector mesons for two values of the three-momentum k: k=0.0 (left panels) and respectively k=0.5 GeV (right panels). In the upper panels the ρ spectral function in nuclear medium with resonant contributions only are displayed for different values of the density parameter. In the lower panel spectral functions are plotted by taking into account progressively the various in-medium contributions discussed in the text at saturation density of nuclear matter. The vacuum spectral functions are also plotted for comparison.

resonance considered, the latter being an energy dependent quantity. In the actual calculations, to determine $\Sigma^{\mu\nu}$ for a particular resonance R, the matrix elements of the RNV vertex provided by the eVMD model described in the previous Section have been used. For the calculation of the dilepton yield in heavy-ion collisions a meson self-energy averaged over the transversal and longitudinal degrees of freedom will employed, $\Sigma(k,n)$=(2 Σ^T(k,n)+Σ^L(k,n))/3, which can be used in Eq. (9) instead of $\Pi^{L,T}$ to obtain an average spectral function $A(k_0,\vec{k})$.

Similar expressions to Eq. (11) are obtained for the contributions due to non-resonant Compton scattering of vector mesons off nucleons (see Fig. (1)a)-b)). The couplings of ρ and ω vector mesons to nucleons were chosen to be

$$\mathcal{L}_{NN\rho} = g_\rho^V\,\overline{\psi}\gamma^\mu\,\vec{\tau}\,\psi\cdot\vec{\rho}_\mu + \frac{ig_\rho^T}{4m_N}\,\overline{\psi}\,\sigma^{\mu\nu}\,\vec{\tau}\,\psi\cdot(\partial_\mu\vec{\rho}_\nu-\partial_\nu\vec{\rho}_\mu)\,, \tag{12}$$

$$\mathcal{L}_{NN\omega} = g_\omega^V\,\overline{\psi}\gamma^\mu\psi\omega_\mu\,, \tag{13}$$

the values of the coupling constants reproducing the ones used in the Bonn OBE model for the NN interaction: ${g_\rho^V}^2/4\pi$=0.84, g_ρ^T/g_ρ^V=6.09 and ${g_\omega^V}^2/4\pi$=20.00. The only difference with relations Eq. (11) resides in the fact that each of the contribution is now multiplied with a step function: $\theta(|\vec{p}+\vec{k}|-p_F)$ and respectively $\theta(|\vec{p}-\vec{k}|-p_F)$ as a result of Pauli blocking of the scattered on nucleons. As an effect, the sum of the two contributions is not gauge invariant anymore, as opposed to the vacuum case. The third and last in-medium contribution to the vector mesons self-energies is due to scattering of mesons off nucleons with the exchange of σ mesons as in Fig. (1)c). The Bonn σNN interaction with $g_\sigma^2/4\pi$=6.73 is used, while the $\rho\rho\sigma$ vertex is described by the effective Lagrangian

$$\mathcal{L}_{\rho\rho\sigma} = -g_{\rho\rho\sigma}(\partial_\mu\vec{\rho}_\nu-\partial_\nu\vec{\rho}_\mu)\cdot(\partial^\mu\vec{\rho}^\nu-\partial^\nu\vec{\rho}^\mu)\,\sigma\,. \tag{14}$$

The coupling constant $g_{\rho\rho\sigma}$ is determined by requiring that the value of the branching ratio $B(\rho^0\rightarrow\pi^+\pi^-\pi^+\pi^-)$=$(1.8\pm0.9)\times10^{-5}$ is reproduced supposing that the mentioned decay is a two-step process: $\rho^0\rightarrow\rho^0\sigma\rightarrow\pi^+\pi^-\pi^+\pi^-$. A similar interaction is supposed to exist for the ω meson with $g_{\omega\omega\sigma}=3g_{\rho\rho\sigma}$.

We turn now to quantitative results for the spectral functions of the ρ and ω vector mesons. In obtaining the present results the following set of nucleonic resonances has been considered: $N^*(1440), N^*(1520), N^*(1535), N^*(1650), N^*(1680), \Delta^*(1232), \Delta^*(1620), \Delta^*(1700)$ and $\Delta^*(1905)$. In Fig. (2)(left) we present results for the ρ meson average spectral function $A(k_0,\vec{k})$ introduced before for two values of the meson three-momentum k: k=0.0 GeV which corresponds to a meson at rest with respect to nuclear matter and k=0.5 GeV. In the upper plots results at various nuclear matter densities: $1/2\rho_0$, ρ_0, $2\rho_0$ are presented by including only contributions from nucleonic resonances to the in-medium self-energies and compared with vacuum. It is readily visible that with the increase of density the original Breit-Wigner peak gets broader and shifted towards higher invariant masses, an effect mainly due to contributions from the Δ resonances with a mass higher than 1600 MeV.

In-medium contributions are most readily visible in a secondary peak at invariant masses around 0.5 GeV or below, originating in the excitation from excitation of N*(1520), N*(1535), and Δ(1620). Its magnitude increases with increasing density, as one would expect from the low density theorem and displays a strong dependence on the value of meson's three-momentum. The hadronic models of Post *et al.*[21] and Lutz *et al.*[8] provide a similar picture, up to a quantitative agreement of the former model due to a similarity in both the approach and included physics. The latter model relies on a dynamic generation of nucleonic resonances within a relativistic and unitary approach to pion and photo-nucleon reactions and as a result the decay width of the N*(1520) resonance is roughly an order of magnitude smaller than the listed PDG vacuum value having as a result a rather small impact of nucleonic resonances on the vector meson spectral functions at small invariant masses. In the lower part of Fig. (2) the importance of the non-resonant contributions to in-medium spectral functions at nuclear-matter saturation density is studied by adding these terms progressively to the final result. The non-resonant Compton scattering contribution increases with the meson three-momentum leading to a shift of the original meson branch towards lower invariant masses and increasing the decay width somewhat. Inclusion of σ meson exchange terms leads to a similar effect.

In a subsequent plot, Fig. (2)(right), our results for the ω meson are presented in an identical display as for the ρ meson. A strong influence of resonant contributions is observed, already at densities well below the nuclear matter saturation density with results in the appearance of a sharp (30$\div$100 MeV) second branch in-medium at invariant masses of less than 0.5 GeV. This is mainly due to excitation of N*(1535) and N*(1520) in the order of importance. The original peak shifts towards slightly higher masses with a decay width of about an order of magnitude higher than in vacuum and strength comparable to the newly observed second branch. Qualitatively the models of Post *et al.*[21] and Lutz *et al.*[8] agree with our findings, with the exception the strength of second ω branch is considerably smaller relatively to the original peak. The inclusion of the non-resonant terms has as main effect a a shift of the original ω peak towards smaller masses supplemented by a strong suppression. Consequently, in nuclear medium, the ω vector meson survives as a quasi-particle of lower mass than in vacuum (300$\div$400 MeV) due to excitation of nucleonic resonances.

III. UNCERTAINTIES IN THE THEORETICAL PREDICTIONS

Theoretical predictions suffer from uncertainties originating from various sources. In this section we will concentrate on two such sources, which have ultimately to do with our limited capabilities to both measure physical observables (otherwise stated, the input of theoretical models suffer from the limited resolution of experimental setups) and model physical processes. First we will study the sensitivity of our predictions for the in-medium meson spectral functions and dilepton spectrum on the values of the eVMD coupling constants. Secondly we will investigate to what extent the momentum distribution in the fireball created during a heavy-ion collisions affects observables such as mass distribution of emitted dileptons. Due to limited space we have omitted to present details on both the microscopical model describing the elementary dilepton production reactions and the transport model (QMD) used to simulate heavy-ion collisions. We refer the interested reader to [14, 20].

A. Coupling constants

The free parameters of the eVMD model, C_{1i}, C_{2i} and C_{3i} (see Eq. (4)), have been extracted by performing a χ^2 fit to the "experimental" values of the helicity amplitudes $A_{1/2}$, $A_{3/2}$ and $S_{1/2}$, which were extracted, in a model dependent way, from the experimentally accessible observables in reactions such as $\gamma N \to \pi N$. As such, these quantities are affected by the finite precision with which experimental measurements are performed, the end results being subject quite often to sizeable relative errors. We will exemplify with the case of the nucleonic resonances N(1520) and N(1535). The former has been determined to give the dominant contribution to vector-meson in-medium self-energies at invariant masses close to 0.5 GeV (see the previous Section), while the latter gives important contributions to dilepton emission, due to is sizable coupling to the ω meson, via the reaction $N(1535) \to \omega + N \to e^+e^- + N$. In the Particle Data Booklet the following values for the $A_{1/2}$ helicity amplitude are quoted: for $N(1520) \to \gamma + p$ $A_{1/2} = -0.024 \pm 0.009 GeV^{-1}$ and for $N(1535) \to \gamma + p$ $A_{1/2} = 0.090 \pm 0.030 GeV^{-1}$ which indicate that quite often the extracted values of the $A_{1/2}$, $A_{3/2}$ and $S_{1/2}$ amplitudes from experimental data is accompanied by large uncertainties. Taking into account the accepted errors for each of the helicity amplitudes involved in the extraction of the coupling parameters mentioned above, we have determined, following a χ^2 fit procedure, the precision at which these parameters have been extracted from the available data. Once again, we only present results for the N(1520) and N(1535) resonances, the situation being similar for each of the resonances considered in the eVMD. As is can be seen from Tab. (I) sizable relative errors can affect some of the coupling parameter, in accordance with one's expectation.

Resonance	C_{10}	C_{11}	C_{20}	C_{30}
N(1520)	2.176±0.020	-1.234±0.200	-1.974±0.100	-0.166±0.250
	0.220±0.050	1.876±0.060	-0.315±0.100	-0.230±0.030
N(1535)	0.662±0.140		-0.208±0.005	
	-0.229±0.070		0.200±0.040	

TABLE I: Couplings constant of the N(1520) and N(1535) resonances in the eVMD in the isospin 0 and isospin 1 channels together with the uncertainties resulting from an imprecise knowledge of the fitted helicity amplitudes $A_{3/2}$, $A_{1/2}$ and $S_{1/2}$.

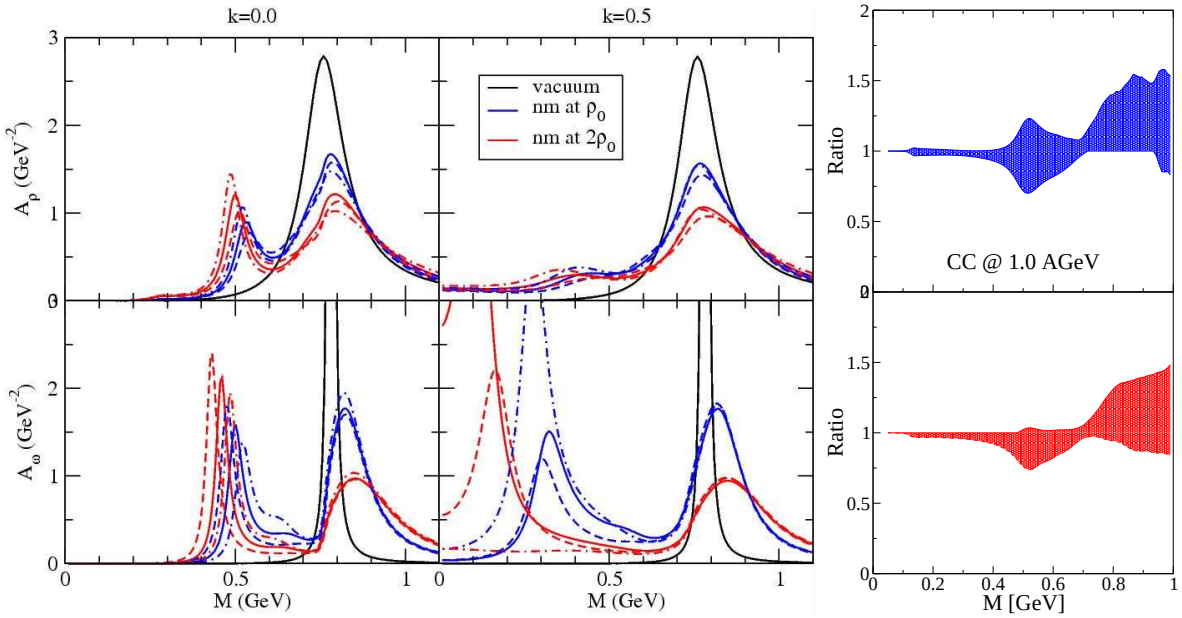

FIG. 3: Sensitivity of the in-medium vector meson spectral functions with respect to variation of the eVMD coupling parameters within one standard deviation (left plot). Right side plot depicts the relative variation of the predicted dilepton spectum for CC at 1.0 AGeV (upper panel) and 2.0 AGeV (lower panel) due to the same variation.

It is worth mentioning that the quoted values for the size of the error bars correspond to one standard deviation which translates into a 65% confidence level. For a higher level of confidence the error bars have to be increased accordingly.

The natural question is to what extent are our conclusions regarding the vector meson in-medium properties affected by the above consideration and what is the sensitivity of the dilepton spectrum to these variations. Both questions are answered by the plots in Fig. (3). The left plot presents the sensitivity of the in-medium ρ and ω spectral functions when the eVMD coupling parameters are varied within 1σ bounds for two nuclear matter densities: ρ_0 and $2\rho_0$ depicted by the blue and red curves respectively. One feature is readily observed: the original mass-branch of the vector meson is slightly affected, while the secondary branch, due to the excitation of nucleonic resonances in-medium is affected to the extent to which one cannot discriminate between phenomena taking place at densities ρ_0 or 2ρ. This affects the use of vector mesons as effective probes of the high-density nuclear matter formed during heavy-ion collisions. In the right plot of Fig. (3) we study to what extent these uncertainties affect the dilepton spectrum, by plotting the ratio between the dilepton emission cross-section varying the eVMD couplings within the 1σ bounds and the cross-section for the central values of those parameters. Results are presented for the C+C system at two colliding energies: 1.0 AGeV (upper panel) and 2.0 AGeV (lower panel). The sensitivity is present at invariant mass of 0.4 GeV or more, at lower energies the dilepton spectrum is dominated by the Dalitz decay of the π_0 and η mesons which are of course not affected by the present considerations. At both colliding energies the ratio increases with the invariant mass, and the presented results indicate an uncertainty in the dilepton emission cross-section of roughly 50% over the whole mass range. This value would increase if one would aim for a higher confidence level.

B. Finite nuclear matter

A second source for uncertainties for the in-medium vector meson spectral functions and the dilepton spectrum originates from the momentum distribution of nucleons in the fireball created during the heavy-ion collision. In Eq. (11) it is tacitly assumed that nucleons are uniformly distributed as a function of momentum between p=0 and p=p_F with no contributions from above the Fermi-see level. This corresponds to the assumption that vector mesons are produced and propagate in an infinite nuclear matter system at equilibrium. In practice, the fireball created during the collision process, is most certainly far from equilibrium and finite. The infinite nuclear matter approximation might therefore be a rather crude approximation in the case when a meaningful comparison between the theoretical dilepton spectrum and the measured one is desired. To study the effect of this approximation on the observables of interest, instead of the infinite nuclear matter approximation, we will take the other possible extreme limit: finite nuclear matter at equilibrium, namely we will employ the momentum distribution of nucleons inside finite nuclei. For that we will make use of the results presented in [25], where the momentum distribution inside finite nuclei is extracted by solving a Dyson equation for the single-particle Green's function

$$\begin{aligned} g(p,\omega) &= g^{(HF)}(p,\omega) + g^{(HF)}(p,\omega)\,[\,\Sigma^{(2p1h)}(p,\omega) + \Sigma^{(2h1p)}(p,\omega)\,]\,g^{(HF)}(p,\omega) \\ g^{(HF)}(p,\omega) &= \frac{\Theta(p_F-p)}{\omega-\varepsilon_p-i\eta} + \frac{\Theta(p-p_F)}{\omega-\varepsilon_p+i\eta}\,. \end{aligned} \tag{15}$$

The contributions to the in-medium nucleon self-energies are depicted in the left plot of Fig. (4). Once the single particle Green's function g(k,ω) is known the momentum distribution $n(k)$ can easily be calculated from its imaginary part by

$$n(p) = \frac{1}{\pi}\int_{-\infty}^{\varepsilon_F} d\omega Im\, g(p,\omega)\,. \tag{16}$$

The results of such an exercise are plotted in the right-side plot of Fig. (4) for both the momentum and energy distributions. The authors have provided results for two choices of the effective nucleon-nucleon interaction: a one-boson exchange potential (Bonn) and a Reid soft-core potential. We will make use of the results for the former choice of interaction. To accommodate for a non-trivial momentum distribution in the fireball, the measure of the integrals in Eq. (11) has to be changed $d^3\vec{p} \longrightarrow d^3\vec{p}\,n(p)$ at the same time with replacing the integrals upper limit p_F with infinity. The results presented in [25] have been calculated for a medium density equal to ρ_0. We use their results by supposing that a density different from ρ_0 the following scaling property of the momentum distribution function $n(p)$ is valid: $n(p/p_F)|_\rho$=$n(p/p_F)|_{\rho_0}$. This is obviously a rather crude approximation.

In Fig. (5) left-side plot results regarding the sensitivity of the spectral function to the fireball momentum distribution are presented. We show again results at two different densities of the nuclear medium: ρ_0 and $2\rho_0$. Results for the infinite nuclear matter are labelled with 'nm' and depicted by full curves, while for finite nuclear matter ('fnm') are represented by the dashed curves. Both the original mass branches and the excited resonance mass branches show considerable sensitivity to the momentum distribution in the fireball, results for the densities $\rho = \rho_0$ and $\rho = 2\rho_0$ being practically indistinguishable for most of invariant mass region considered. It is worth noting that the position of the secondary mass branch can be extracted, due to these uncertainties, with a precision of only 200-300 MeV. The right-side plot of Fig. (5) presents the relative changes in the dilepton spectrum as a result of considering a nucleon momentum distribution specific to finite nuclear matter in equilibrium. Results are show for the C+C system at incident energies of 1.0 AGeV (blue curve) and 2.0 AGeV (red curve) for the ratio between emission cross-section in finite nuclear matter and emission cross-section in infinite nuclear matter. Results indicate that due to the different nucleon momentum distribution dilepton emission can be suppressed by up to 50% compared with the infinite matter case. This result should not be taken ad literam, but only as an indication that momentum distribution in the fireball can have an important effect on observables such as emitted dilepton spectra and as a consequence a fully consistent treatment would be the inclusion of in-medium effects together with dilepton degrees of freedom already at the level of the transport model used in simulating the heavy-ion collision process.

IV. DILEPTON SPECTRUM

In this Section we provide theoretical predictions for dilepton emission in C+C collisions at 1 and 2 AGeV. The main purpose will be to compare calculations that include in-medium effects in a more traditional way, *i.e.* via Brown-Rho scaling of the vector meson masses and empirical collisional broadening of the decay widths, with preliminary results obtained using ρ and ω mesons described by the in-medium spectral functions of the previous Section II. Our results are shown in Fig. (6).

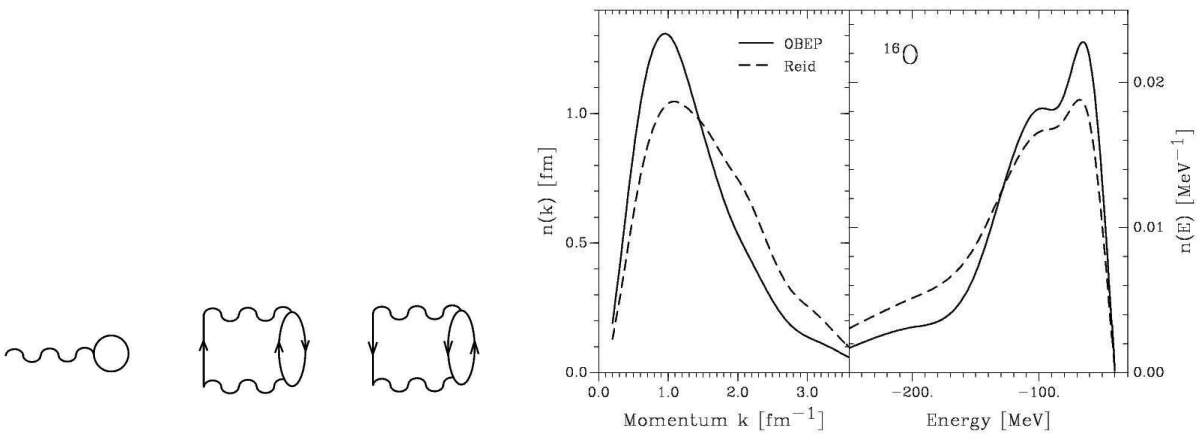

FIG. 4: Diagrammatic representation of the Hartree-Fock, the 2-particle 1-hole and 2-hole 1-particle contributions to the nucleon self-energy in-nuclear medium (left plot) taken into account in [25]. The right hand side plot presents the single-particle density in a light nucleus (^{16}O as a function of momentum (left panel) and energy (right panel).

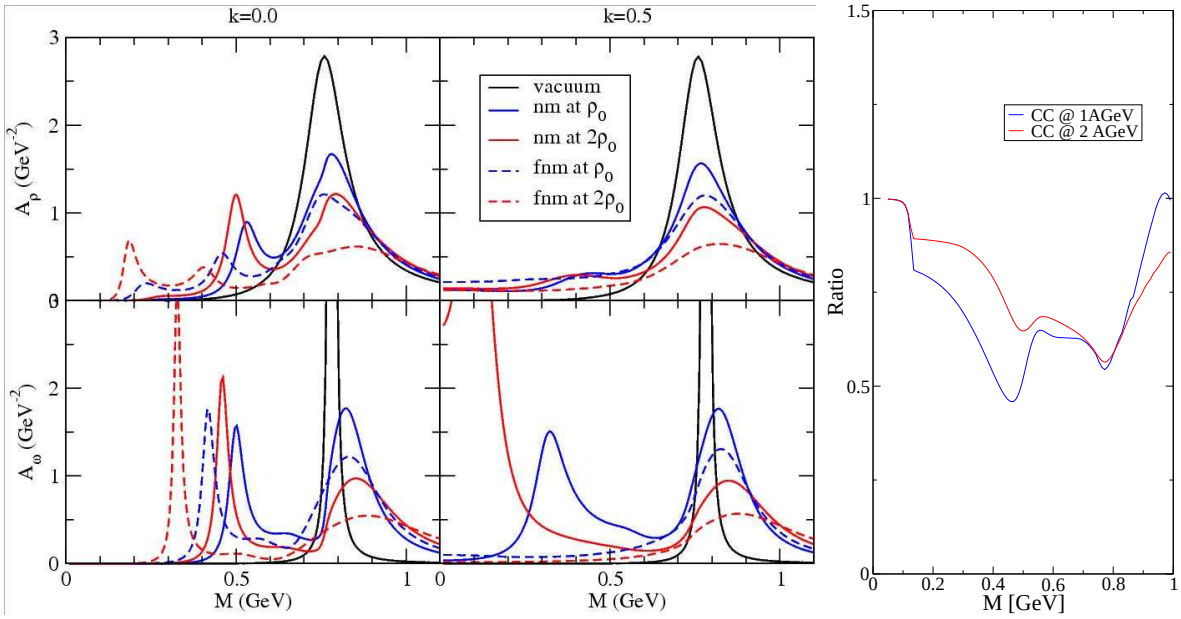

FIG. 5: In-medium meson spectral function variation as a results of changing the nucleon momentum distribution from a infinite matter to a finite matter one. The relative effect of such a process on the dilepton spectrum emitted during C+C collisions is shown in the right side plot.

Dilepton spectra at intermediate energies (probed by DLS and HADES experiments) are more sensitive to the ω meson collisional broadening. In absence of in-medium modifications of mesons the invariant mass dilepton spectrum would show a pronounced ω peak (black curve in Fig. (6)). In the DLS experiment such an enhancement has not been observed. Despite the limited mass resolution in [14] an in-medium ω width of $\Gamma_\omega^{tot} = 100 \div 300$ MeV at nuclear matter density $\rho = 1.5\rho_0$ has been extracted from the DLS data. The modification of the ρ width was found to be similar in magnitude, i.e. $\Gamma_\rho^{\rm tot} = 200 \div 300$ MeV (again at $\rho = 1.5\rho_0$).

For the Brown-Rho scaling/collisional broadening scenario we present calculations with an assumed linear dependence of the ρ and ω decay widths, i.e. $\Gamma_V^{\rm tot} = \Gamma_V^{\rm vac} + \rho/\rho_0 \Gamma_V^{\rm coll}$, with $\Gamma_\omega^{\rm tot}$=125 MeV, $\Gamma_\rho^{\rm tot}$=250 MeV at $\rho = \rho_0$. Simultaneously, the masses of mesons are supposed to vary as a function of the nuclear matter density at the point where the resonance decay occurs, following a Brown-Rho scaling law $m_V^* = m_V(1 - \alpha\rho/\rho_0)$ with ρ the local baryon density and $\alpha = 0.2$. Results are indicated by the red curve in Fig. (6). This calculation also includes contributions of an additional in-medium effect, decoherence, which has as a result an increase of the dilepton production cross-section with roughly %50 at intermediate masses [20]. Sensitivity of the dilepton spectrum with respect to variations of the

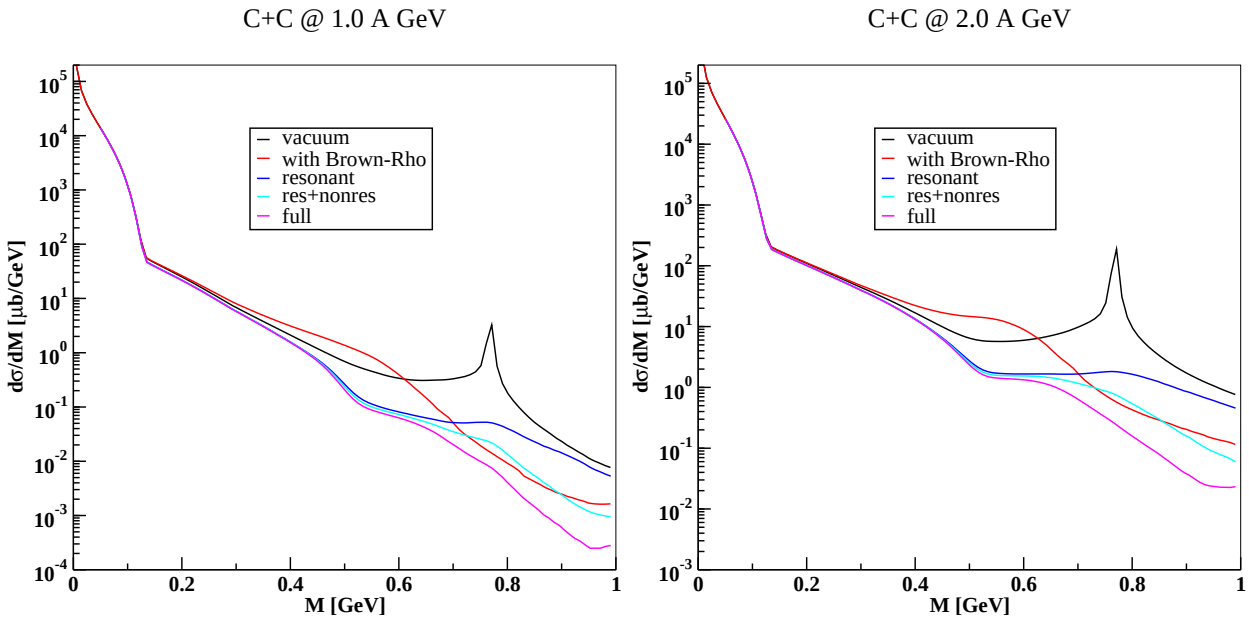

FIG. 6: Dilepton spectrum in C+C at 1.0 AGeV (left panel) and 2.0 AGeV (right panel). Brown-Rho scenario calculations are depicted by the red curve. Results obtained using the spectral function approach for vector mesons are represented by the blue, cyan and magenta curve (see text for details). The vacuum result (black curve) is shown for comparison.

ρ and ω collisional widths is mild [20]: variation of $\Gamma_\rho^{\rm tot} = 150 \div 250$ MeV leads to a modification of the dilepton yield by a factor of 2 in the dilepton mass range 0.5-0.8 GeV, while a calculation with a moderately low value for the ω widths $\Gamma_\omega^{\rm tot}$= 60 MeV allows for at most %50 increase in the same mass region.

Medium effects can enter in a few places in the expression for the dilepton production rate. As the decay of a resonance into a dilepton pair runs through an intermediate vector meson (within the VMD approach) the branching ratio $dB(s,M)^{R\to VN\to Ne^+e^-}/dM^2$ is expected to alter. Medium modification will affect both $d\Gamma(s,M)^{R\to VN\to Ne^+e^-}/dM^2$ and $\Gamma(s)^{R\to \rm anything}$. The former is accounted for by including in the expression of the vector mesons propagators the effect of the in-medium self-energies. This procedure only affects the ground state ρ and ω vector mesons, their excited states are supposed to be, in a first approximation, unaffected by the presence of the dense nuclear medium. In-medium modifications of the total decay widths of nucleonic resonances occur due to in-medium modifications of the vector mesons and Pauli blocking of nucleons. At present we have only partially accounted for the first source, *i.e.* the meson spectral functions with the provision that the total resonance decay widths have not been iterated (as they depend upon each other) to obtain self-consistency.

We present in Fig. (6) theoretical predictions for the dilepton spectrum within the spectral function approach to in-medium vector mesons for three scenarios of in-medium effects: first we only include contributions from nucleonic resonances to in-medium meson self-energies (blue curve) and than gradually add non-resonant Compton scattering (cyan curve) and finally also σ meson exchange contributions (magenta curve). For these curves the emission of dileptons due to Dalitz decays of pions and η mesons does not change. Substantial difference with respect to the traditional Brown-Rho/collisional approach is observed over the while mass range. At invariant masses below 0.7 GeV the dilepton production rate has decreased by a factor up to 10 due to a strong decrease of the dilepton emission through decays of nucleonic resonances in this mass region, most notably the $\Delta(1232)$ isobar. The effect is more pronounced for the 2 AGeV C+C reaction, since previously the Dalitz η and nucleonic decays were of comparable magnitude, while for the 1 AGeV case the latter dominates. At invariant masses above 0.7 GeV the outcome of the three consired in-medium scenarios vary widely. Inclusion of only nucleonic resonance contribution leads to an important increase of the dilepton cross-section in this region with respect to the old case, while the inclusion of non-resonant background suppresses the dilepton spectrum quite strongly.

V. FINAL CONCLUSIONS

We have presented results for the in-medium spectral functions of the ρ and ω vector mesons. Interactions between vector mesons and nuclear matter were described using the eVMD model. Important modifications of meson properties

with respect to vacuum are observed due to the excitation of nucleonic resonances in nuclear matter: the original Breit-Wigner peak gets broader and shifts towards higher masses. As second peak, due to excitation of nucleonic resonances, is observed at low invariant masses. A strong dependence on the meson three-momentum has also noticed been noticed. Inclusion of additional in-medium contributions (non-resonant Compton scattering and σ meson exchange contributions) results in a downward shift of the main mass branch and an additional increase of the collision width for the ρ. For the ω meson the results are more dramatic: the original peak dissolves while the secondary branch due to resonance excitations is narrow enough (30-100 MeV) to allow this meson to keep its quasi-particle properties in-medium.

Additionally the sensitivity of the in-medium spectral functions and dilepton spectrum with respect to variation of the coupling parameters of the eVMD model and different momentum distribution of the nucleon in the fireball have been studied. The former reveals an important sensitivity of the secondary mass branches of vector mesons in medium and about %50 change in the dilepton spectrum at one standard deviation level for the couplings. For the latter the outcome is somewhat more important: spectral function are sizably affected over the whole range of invariant masses while the change in the dilepton spectrum can amount up to a factor of 2. This might indicate that the inclusion of in-medium effects together with the elementary dilepton emission processes at the level of the transport model is mandatory.

Finally, a comparison of the dilepton spectral in C+C heavy-ion collisions by including in-medium effects in a traditional way (Brown-Rho mass scaling and collisional broadening for vector mesons) and within a many-body approach has been performed. An important difference between the two approaches is observed at invariant masses of about 0.5 GeV, which also coincides with the region were a comparison with the recently available HADES experimental data fails. Taking into consideration the discussed uncertainties in the theoretical spectra (from the sources discussed above and possibly others) it might be possible to alleviate this discrepancy. Other alternative might be the inclusion of additional dilepton production channel, originally thought to be of little importance, but recently suggested by other authors to have been underestimated [26](pn bremsstrahlung). Work in this direction is in progress.

---

[1] G.E. Brown and M. Rho, Phys. Rev. Lett. **66**, 2720 (1991); Phys. Rep. **269**, 333 (1996).
[2] T. Hatsuda and S.H. Lee, Phys. Rev. C **46**, R34 (1992); S. Leuopold, *ibid.* **64**, 015202 (2001);
[3] C.M. Shakin and W.D. Sun, Phys. Rev. C **49**, 1185 (1994); M. Asakawa and C.M. Rho, Phys. Rev. C **48**, R526 (1993).
[4] M. Post, S. Leupold, and U. Mosel, Nucl. Phys. A **741**, 81 (2004).
[5] D. Cabrera, E. Oset, and M.J. Vicente Vacas, Nucl. Phys. A **705**, 90 (2002).
[6] F. Klingl, N. Kaiser, and W. Weise, Nucl. Phys. A **624**, 527 (1997).
[7] K. Saito, K. Tsushima, and A.W. Thomas, arXiv:nucl-th/98110311.
[8] M.F.M. Lutz, G. Wolf, and B. Friman, Nucl. Phys. A **706**, 431 (2002).
[9] P. Muehlich, V. Shklyar, S. Leupold, U. Mosel, and M. Post, Nucl. Phys. A**780**, 187 (2006).
[10] R.J. Porter *et al.* [DLS Collaboration], Phys. Rev. Lett. 79, 1229 (1997).
[11] W.K. Wilson *et al.* [DLS Collaboration], Phys. Rev. **C57** (1998) 1865.
[12] E.L. Bratkovskaya, W. Cassing, R. Rapp, and J. Wambach, Nucl. Phys. A **634**, 168 (1998).
[13] C. Ernst, S.A. Bass, M. Belkacem, H. Stocker, and W. Greiner, Phys. Rev. C **58**, 447 (1998);
[14] K. Shekter, C. Fuchs, A. Faessler, M. Krivoruchenko, and B. Martemyanov, Phys. Rev. C **68**, 014904 (2003).
[15] R. Arnaldi *et al.* [NA60 Collaboration], Phys. Rev. Lett. **96** (2006) 162302.
[16] J. Friese, HADES Collaboration, Prog. Part. Nucl. Phys. **42**, 235 (1999).
[17] A. Faessler, C. Fuchs, and M.I. Krivoruchenko, Phys. Rev. C **61**, 035206 (2000).
[18] M.I. Krivoruchenko, B.V. Martemyanov, A. Faessler, and C. Fuchs, Ann. Phys. **296**, 299 (2002).
[19] A. Faessler, C. Fuchs, M.I. Krivoruchenko, and B.V. Martemianov, J. Phys. G **29**,603 (2003).
[20] M.D. Cozma, C. Fuchs, E. Santini, and A. Faessler, Phys. Lett. B **640**, 170 (2006).
[21] M. Post and U. Mosel, Nucl. Phys. A **688**, 808 (2001).
[22] A.I. Vainstein and V.I. Zakharov, Phys. Lett. B**72**, 368 (1978).
[23] S.J. Brodsky and G.R. Farrar, Phys. Rev. C **11**, 1309 (1975);
[24] C. Fuchs, M.I. Krivoruchenko, H. Yadav, A. Faessler, B.V. Martemyanov, and K. Shekther, Phys. Rev. C **67**,025202 (2002).
[25] H. Müther, G. Knehr and A. Polls, Phys. Rev. C **52**, 2955 (1995).
[26] E. Bratkovskaya, *Dileptons from heavy-ion collisions: from SIS to FAIR and off-shell transport*, talk given at the workshop "Electromagnetic probes for strongly interacting matter: the quest for medium modifications of hadrons", Trento, Italy (2007).